EURASIAN PHYSICAL TECHNICAL JOURNAL

2024, Volume 21, No. 1 (47)

https://doi.org/10.31489/2024No1/84-92

Received: 29/12/2023 Revised: 26/01/2024 Accepted: 24/02/2024 Published online: 29/03/2024
Research Article

UDC: 533.6.011, 621.453, 519.63

EFFECT OF TWO-PHASE FLOW ON THE FUEL GRAIN IGNITION AND ITS DEPARTURE FROM THE CARTRIDGE CASE

Minkov L.L., Gimayeva N.R.

National Research Tomsk State University, Tomsk, Russia
*Corresponding author: lminkov@ftf.tsu.ru

Abstract. *False heat targets play an important role in the safety of aircraft and helicopters. The main task is to ensure stable ignition of the fuel grain before leaving the cartridge case. In order to optimize this process, it is important to study the influence of various parameters, such as the size of the gap between the cartridge case and the cylindrical surface of fuel grain, as well as the size of the particles coming from the initiator and fuel grain. This article offers a physical and mathematical model of the ignition and departure process of the grain, and studies the influence of the specified parameters on the ignition time. The ignition times of the grain end surface for different particle sizes equals r = 1 μm and r = 25 μm have been estimated, the gap between the cartridge case and the cylindrical surface of grain ranged from 0.5 mm to 2 mm. The output velocities of the grain from the cartridge case are obtained for particles equal to 1 μm and 25 μm and different gap between the cartridge case and the cylindrical surface of fuel grain.*

Keywords: false heat targets, combustion, combustion products, mathematical modeling, muzzle velocity, internal ballistics

1. Introduction

Systems known as false heat targets play an important role in ensuring promotion of safety of fixed wing aircraft and helicopters flights on various missions [1]. False heat targets are devices capable of emitting a large amount of heat during propellant mixture combustion, which prevents detection of the exact location of the aircraft whose engine temperature is high [2].

False heat targets are similar to the ammunition of signal or illuminating launchers [3] and consist of a cartridge case filled with solid fuel composition. The successful use of false heat targets requires the stable ignition of the pyrotechnic composition of the fuel grain before it leaves the cartridge case [4].

In order to achieve full ignition of the end part of the fuel grain while it is in the cartridge case, it is necessary to identify the influence of various parameters on the ignition process and the grain discharge from the cartridge case. Within the framework of this task, it is necessary to determine the optimal design parameters, such as the size of the gap between the cylindrical surfaces of the cartridge case and grain, as well as the size of the particles coming from the initiating device and the pyrotechnic composition of the fuel grain. Information about the impact of these parameters on the ignition process is important to minimize the possibility of false start-ups.

The purpose of this article is to develop a physic-mathematical model of the process of ignition and departure of the fuel grain from the cartridge, to study the influence of the particle size coming from the initiating device and the pyrotechnic composition of the grain, the gap between the cartridge case and the cylindrical surface of fuel grain on the ignition time of the end grain surface.

2. Physical statement of the problem

The fuel grain 3 in cartridge case 2 is shown in Figure 1. The cartridge case at one end is closed by a membrane 4, which opens when the shot-start pressure is reached. At the initial time, combustion products consisting of the initiator gas and inert particles are received from the initiator's surface 1. Between the grain surface and the combustion products there is heat exchange due to radiation, particle conduction and convection of combustion products. When the grain surface reaches the ignition temperature, combustion products consisting of fuel grain gas and particles enter the cartridge case free volume. At the moment when boosting pressure is reached on the membrane, the membrane opens. In this case, under the influence of the dynamic pressure of combustion products flowing from the free volume, the grain begins to move along the *x* axis and leaves the cartridge case.

This article considers the research of process within the following assumptions. The combustion products flow is two-dimensional axisymmetric, the combustion products are a viscous compressible multi-temperature and multispeed medium [5] consisting of a multi-component gas (air, initiator gas and grain gas) and particles of the initiator and particles of the grain.

To estimate the time of the grain ignition, the problem of involving the fuel grain surface to the burning is solved. It is assumed, that the ignition of the surface, i.e. its inclusion in the combustion process, occurs gradually after the temperature at a given point has reached some critical value. The surface temperature is usually found either by numerically solving the non-stationary thermal conductivity equation [6, 7] or by solving the ordinary differential equation [8] obtained by one of the integral methods [9, 10]. This work uses the second method as less resource-intensive.

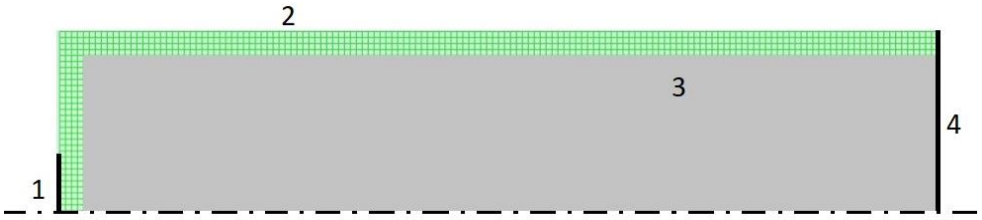

Fig.1. Product appearance: 1 – initiator, 2 – cartridge case, 3 – fuel grain, 4 – membrane

The process of fuel grain movement in the cartridge case is modeled using the equation of motion and dynamic mesh technique.

3. Governing equations

The movement of the fuel grain is modelling with the next system of equations:

$$\frac{dV_t}{dt} = \frac{1}{m_t}\left(2\pi \int_0^{y_1} y p_t dy - \pi y_1^2 p_и\right), \frac{dX_t}{dt} = V_t, \tag{1}$$

With initial conditions: $t = 0$, $V_t = 0$, $X_t = x_1$; где m_t - the mass of grain, p_t - the pressure on the left end of the grain, p_{out} - the pressure outside the cartridge case.

The system of equations describing the gas-dynamic processes occurring inside the free volume of the cartridge case can be written as:

$$\frac{\partial \mathbf{U}}{\partial t} + \nabla \cdot \mathbf{F} = \mathbf{S} \tag{2}$$

The components of the column-vectors U, F, S are presented in Table 1.

Table 1. Components of column-vectors of the system of equations (2)

	U	F	S
Continuity equation for gas	ρ_g	$\rho_g \mathbf{V}_g$	$(1-z_2)\cdot \dot{m}_T$
Equation for the i^{th} gas component	$\rho_g Y_i$	$\rho_g \left(\mathbf{V}_g Y_i - D_{i,eff}\nabla Y_i\right)$	$\begin{cases} 0, & i=1 \\ (1-z_2)\cdot \dot{m}_T, & i=2 \end{cases}$
Momentum equation for gas	$\rho_g \mathbf{V}_g$	$\rho_g \mathbf{V}_g \mathbf{V}_g - \bar{\boldsymbol{\tau}}_{eff,g}$	$\sum_{s=1}^{2} \mathbf{R}_{sg} - \alpha_g \nabla p$
Energy conservation equation for gas	$\rho_g E_g$	$\rho_g \mathbf{V}_g H_g - \bar{\boldsymbol{\tau}}_{eff,g}\cdot \mathbf{V}_g - \alpha_g \lambda_{eff,g}\nabla T$	$-p\frac{\partial \alpha_g}{\partial t} + \sum_{i=1}^{3} h_{i,g}\rho_g D_{i,eff}\nabla Y_i + \sum_{s=1}^{2}\left(Q_{sg} + \mathbf{R}_{sg}\mathbf{V}_g\right) + c_{p,g}T_{P2}(1-z_2)\cdot \dot{m}_T$
Continuity equation for the particles s^{th} fraction	ρ_s	$\rho_s \mathbf{V}_s$	$\begin{cases} 0, & s=1 \\ z_2 \dot{m}_T, & s=2 \end{cases}$
Momentum equation for the particles s^{th} fraction	$\rho_s \mathbf{V}_s$	$\rho_s \mathbf{V}_s \mathbf{V}_s - \bar{\boldsymbol{\tau}}_{eff,s}$	$-\mathbf{R}_{sg} - \alpha_s \nabla p$
Energy conservation equation for the particles s^{th} fraction	$\rho_s H_s$	$\rho_s \mathbf{V}_s H_s - \bar{\boldsymbol{\tau}}_{eff,s}\cdot \mathbf{V}_s - \alpha_s \lambda_{eff,s}\nabla T_s$	$-p\frac{\partial \alpha_s}{\partial t} - Q_{sg} - \mathbf{R}_{sg}\mathbf{V}_s + \begin{cases} 0, & s=1 \\ c_2 T_{P2} z_2 \dot{m}_T, & s=2 \end{cases}$

Here $\dot{m}_T = \rho_{T2} u_{02} p^{\nu_2}\cdot \delta\left(\mathbf{x}-\mathbf{x}_p\right)\cdot \eta\left(T-T_*\right)$ is the mass burning rate of the fuel grain per volume unit, ρ is the density, $\mathbf{V} = U\cdot \mathbf{i} + V\cdot \mathbf{j}$ is the velocity vector, p is the pressure, α is the volume fraction, Y_i is the mass fraction of the i^{th} gas component, i = 1 is the gas coming from the initiator, i = 2 is the gas coming from the surface of the burning grain, s = 1 is particles coming from the initiator, s = 2 is particles coming from the surface of the burning grain, z_2 is the mass fraction of particles in the grain, ρ_{T2} is the density of the grain composition, u_{02} is the coefficient in the burning law of grain composition, ν_2 is the exponent in the burning law of grain composition, $\delta\left(\mathbf{x}-\mathbf{x}_p\right)$ is Dirac delta function, $\mathbf{x}_p$ is the vector of burning grain surface position, $\eta\left(T-T_*\right)$ is the unit function, T_* is the grain surface ignition temperature.

Ideal gas equation:

$p = \rho_g R T_g$,

$R = \sum_{i=1}^{2} R_i Y_i + \left(1 - \sum_{i=1}^{2} Y_i\right) R_3$ is the gas constant, R_3 is the gas constant of air.

The volume fraction of particles and gas is determined from the relations:

$$\alpha_1 = \frac{\rho_1}{\rho_{10}},\ \alpha_2 = \frac{\rho_2}{\rho_{20}},\ \alpha_g + \alpha_1 + \alpha_2 = 1,$$

where ρ_{s0} is the density of particle material.

Stress tensor is written as:

$$\bar{\boldsymbol{\tau}}_{eff,j} = \alpha_j \mu_{eff,j}\left[\left(\nabla \mathbf{V}_j + \nabla \mathbf{V}_j^T\right) - \frac{2}{3}\nabla\cdot \mathbf{V}_j\cdot \bar{\mathbf{I}}\right],$$

where $j = g$ is gas, $j = s$ are particles, $\bar{\mathbf{I}}$ is unit tensor.

Gas enthalpy $E_g = H_g - \frac{\alpha_g p}{\rho_g}$.

Particle enthalpy $H_s = h_s + \frac{\mathbf{V}_s^2}{2}$, $h_s = h_s^0(T_{ref}) + \int_{T_{ref}}^{T_s} c_s dT$.

Phase interaction $\mathbf{R}_{sg} = K_{sg}\left(\mathbf{V}_s - \mathbf{V}_g\right)$, where $K_{sg} = \frac{18\alpha_s\mu_g}{d_s^2}\left(1 + 0.15\,Re_{sg}^{0.687}\right)$.

Heat-exchange rate between phases $Q_{sg} = \frac{6\alpha_p\lambda_g}{d_s^2}\mathrm{Nu}_{sg}\left(T_s - T_g\right)$,

where $\mathrm{Nu}_{sg} = 2 + 0.6\mathrm{Re}_{sg}^{1/2}\mathrm{Pr}_g^{1/3}$, $\mathrm{Pr}_g = \frac{c_{p,g}\mu_g}{\lambda_g}$

To close the governing equations (2), the SST mixture turbulence model is used.
The system of transport equations for the turbulence model has the form [11]:

$$\begin{aligned}
&\frac{\partial}{\partial t}\left(\rho_m k\right) + \nabla\cdot\left(\rho_m \mathbf{V}_m k\right) = \nabla\cdot\left(\Gamma_k \nabla k\right) + G_k - Y_k + S_k \\
&\frac{\partial}{\partial t}\left(\rho_m \omega\right) + \nabla\cdot\left(\rho_m \mathbf{V}_m \omega\right) = \nabla\cdot\left(\Gamma_\omega \nabla\omega\right) + G_\omega - Y_\omega + S_\omega
\end{aligned}, \qquad (3)$$

where Γ_k and Γ_ω are the effective diffusivity of k and ω, respectively, Y_k and Y_ω are the dissipation of k and ω due to turbulence, G_k is the production of turbulence kinetic energy, G_ω is the generation of ω,

$\mu_{eff,j} = \mu_j + \mu_{t,j}$, $\mu_{t,j} = \frac{\rho_j}{\rho_m}\mu_{t,m}$, $\mu_{t,m} = \rho_m \frac{k}{\omega} a$, $\lambda_{eff,j} = \lambda_j + \frac{c_{p,m}\mu_{t,j}}{Pr_t}$, $D_{eff,i} = D_i + \frac{\mu_{t,i}}{\rho_m Sc_t}$, $\rho_m = \sum_{i=1}^{3}\alpha_i\rho_{i0}$,

$\mathbf{V}_m = \frac{1}{\rho_m}\sum_{i=1}^{3}\alpha_i\rho_{i0}\mathbf{V}_i$, $\mu_m = \sum_{i=1}^{3}\alpha_i\mu_i$, $S_k = k_p \dot{m}_i$, $S_\omega = \omega_p \dot{m}_i$, $k_p = \frac{3}{2}\left(I\frac{\dot{m}_i}{\rho_{m,p}}\right)^2$, $\omega_p = \frac{k_p}{10\nu_{m,p}}$, $\nu_m = \mu_m/\rho_m$.

D_i is the diffusion coefficient of the i^{th} gas component. Index p is related to near wall cell.

The source terms are: $S_{1,g} = 0$, $S_{2,g} = S_{m,g}$, $S_{m,1} = 0$, $S_{m,2} = \frac{z_2}{1-z_2}\cdot S_{m,g}$, $S_{h,g} = S_{m,g}T_{P2}c_{p,g}$, $S_{h,1} = 0$, $S_{h,2} = S_{m,2}T_{P2}c_2$, $\mathbf{V} = U\cdot\mathbf{i} + V\cdot\mathbf{j}$.

Initial condition: $\mathbf{V}_g = \mathbf{V}_s = \mathbf{0}$, $p = p_{in}$, $\rho_g = \rho_{g,н}$, $\rho_s = 0$, $Y_1 = Y_2 = 0$.

Boundary condition:

- wall boundary condition $\nabla Y_i = 0$, $\nabla T = 0$, $\frac{\partial k}{\partial n} = 0$, $\omega = \frac{80\mu_m}{y_p^2\rho_m}$;

  for cartridge case: $\mathbf{V}_g = \mathbf{V}_s = 0$;

  for fuel grain: $\mathbf{V}_g = \mathbf{V}_s = \mathbf{V}_t$, where $\mathbf{V}_t = V_t\cdot\mathbf{i} + 0\cdot\mathbf{j}$;

- outflow boundary condition: $p = p_{out}$, $\frac{\partial\varphi}{\partial n} = 0$, where $\varphi = \{\rho_s, \mathbf{V}_s, H_s\}$, $\frac{\partial^2 k}{\partial n^2} = 0$, $\frac{\partial^2\omega}{\partial n^2} = 0$;

- condition on the axis of symmetry: $V_s = V_g = 0$, $\frac{\partial\varphi}{\partial y} = 0$, where $\varphi = \{\rho, U, H, \rho_s, U_s, H_s, p, Y_i, k, \omega\}$;

- boundary between the initiator and the free volume of the cartridge case: $\rho_g U_g = \left(1 - z_1\right)\cdot\rho_{T1}u_{01}p^{\nu_1}$, $V_g = 0$, $\rho_1 = \frac{z_1}{1-z_1}\cdot\rho_g$, $V_1 = 0$, $U_1 = U_g$, $T_g = T_1 = T_{init}$, $Y_1 = 1$, $Y_2 = 0$, $k = \frac{3}{2}I^2U_g^2$, $\omega = \frac{k}{10\nu_m}$, where: $I = 0.05$.

The temperature of the fuel surface is determined from the solution of the ordinary differential equation obtained by the method of integral ratios by approximating the temperature profile inside the fuel with an exponential function [12]

$$\frac{dT_w}{dt} = \frac{q_w^2}{\lambda_T \rho_T c_T \left(T_w - T_{wn}\right)}, \tag{4}$$

with initial condition:

$T_w\big|_{t=0} = T_{wn}$,

where $q_w = q_{conv} + q_{rad} + q_{cond}$, $q_{conv} = \alpha_{conv}\left(T - T_w\right)$, $q_{rad} = \varepsilon\sigma_0\left(T^4 - T_w^4\right)$, $q_{cond} = \rho_{s0} V_s c_s \left(T_1 - T_w\right)$, ε is the gas emissivity, σ_0 is Stefan-Boltzmann constant, c_s is the heat capacity of the particle substance, $\alpha_{conv} = 0.021\mathrm{Re}^{0.8}\mathrm{Pr}_g^{\ 0.43}\lambda_g / D_{ef}$, $\mathrm{Re} = \rho_g V_{m,g} D_{ef} / \mu_g$, $D_{ef} = 4S/\Pi$ is the effective channel diameter, S is the channel cross section area, Π is the gas-touched channel cross section perimeter.

4. Numerical technique

Layering method (layer generation) was used to simulate the forward movement of the fuel grain in the cartridge case, which completes the calculation grid layers according to the movement of the grain. The result is a computational grid consisting of rectangular cells layers of a given size with a constantly changing number of cells [13]. This type of dynamic mesh is quite simple to implement through user functions in ANSYS Fluent, the application of which allows one to remesh the grid based on the geometry of the model (as a result of solving the equation of motion for the grain) in the calculation process [14].

To solve the system of governing equations, a SIMPLE-like method was used, based on a separate solution of momentum equation for each phase (Phase Coupled SIMPLE) [15]. To approximate the convective parts of the equation, an implicit upwind difference scheme of first order accuracy was used. The PRESTO (PREssure STaggering Option) scheme was used to find pressure on cell faces. Numerical methods for studying viscous gas flows with particles in channels of complex shapes show their effectiveness [16, 17].

5. The discussion of the results

The length of the grain was taken to be 72 mm, the diameter of the initiator was 10 mm, the size of the gap between the end of the grain and the cartridge case was 2 mm, and the diameter of the cartridge case was 30 mm. The size of the gap between the cylindrical surfaces of the grain and the cartridge case varied from 0.5 mm to 2 mm, the particle sizes equal r = 1 μm and r = 25 μm. The membrane boosting pressure was assumed to be 8 atm.

Calculations were carried out using the following data for the initiator igniter composition: $\rho_{T1} = 3220\ kg/\mathrm{m}^3$, $\nu_1 = 0.408$, $u_{01} = 3.74\cdot10^{-4}\ m/(\mathrm{s}\cdot Pa^{\nu_1})$, $z_1 = 0.499$, $T_{P1} = 3430\ K$; for the gas phase: $k = 1.25$, $R_1 = 156.3\ J/(\mathrm{kg}\cdot K)$; for fuel grain pyrotechnic composition: $\rho_{т2} = 1800\ kg/\mathrm{m}^3$, $\nu_2 = 0.4$, $u_{02} = 5\cdot10^{-5}\mathrm{m}/(\mathrm{s}\cdot Pa^{\nu_2})$, $z_2 = 0.681$, $T_{P2} = 2035\ K$, $T_* = 1100\,K$, $\lambda_т = 1.77\ W/(\mathrm{m}\cdot K)$, $c_\mathrm{T} = 1030\ J/(\mathrm{kg}\cdot K)$, for the gas phase: $k = 1.48$, $R_2 = 343\ J/(\mathrm{kg}\cdot K)$.

For analysis the numerical solution for mesh independence, the ignition time t_{ig} of the grain surface end part, which opposite the initiator was chosen as the criterion. Calculations were carried out on a sequence of grids with a step of 1 mm (mesh 1), 0.5 mm (mesh 2) and 0.25 mm (mesh 3). The time step was 10^{-5} s. The height of the gap between the cylindrical surfaces of the grain and the cartridge case was 2 mm, the particle size was chosen r = 1 μm. On grid 1, the ignition time of t_{ig} was 1.3ms, on grid 2 - 1.5ms, on grid 3 - 1.6ms. Finite-difference mesh 2 was chosen for further calculations.

Figure 2 shows gas flux line for various positions of the grain, obtained for a particle radius of 1 μm and a cylindrical gap size of 2 mm. It can be noted, that starting from the moment of time t = 5 ms, a vortex zone is formed between the ends of the cartridge case and the grain, pushed away from the grain end by the combustion products of the grain. As the fuel grain moves towards the exit from the cartridge case, the

vortex zone moves in the same direction, to the left of which a stagnation zone is formed. In the central axial zone of the free volume, a jet flow is formed due to combustion products coming from the initiator.

It will be seen from figure 3, that particles with a radius of 1 μm are carried away by the gas flow and do not accumulate on the fuel grain end surface, which complicates the process of grain heating. Particles with a radius of 25 μm are characterized by sedimentation and accumulation of particles from the initiator at the end of the grain, as well as a more intense heating process of the grain end surface compared to smallest particles.

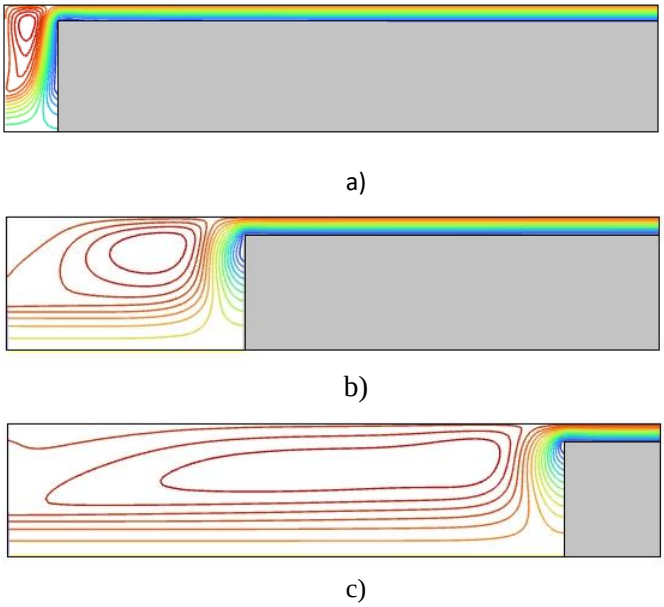

a)

b)

c)

Fig.2. Streamline d=2mm. a) t = 6 ms, b) t = 20 ms, c) t = 40 ms.

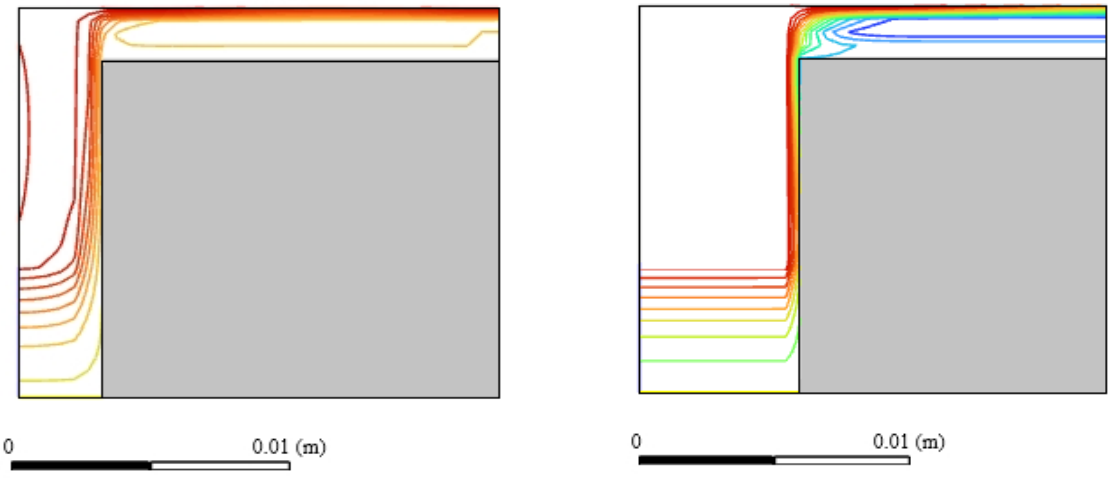

a) b)

Fig.3. Particles trajectory emitted from the initiator at time 5 ms: a) r = 1 μm, b) r = 25 μm

Figure 4 a shows the effect of the size gap between the cylindrical surface of fuel grain and cartridge case on the time ignition of the grain end part for the radius of particles r = 1 μm. The ignition time of the surface part grain, which is located opposite the initiator, is practically independent of the size gap. For the remaining surface part of the grain face, the reducing size gap increases the ignition time. When the radius of the particles is increased to r = 25 μm, (figure 4 b) the effect of the size gap has a slight effect on the ignition time of the grain end face, while the ignition time with a narrower gap is minimal.

Calculations show that increasing of the size gap between the cartridge case and the grain cylindrical part as well as an increasing particle size leads to a decrease in the ignition time of the grain end surface, which is associated with more favorable heat exchange conditions between the combustion products and the grain.

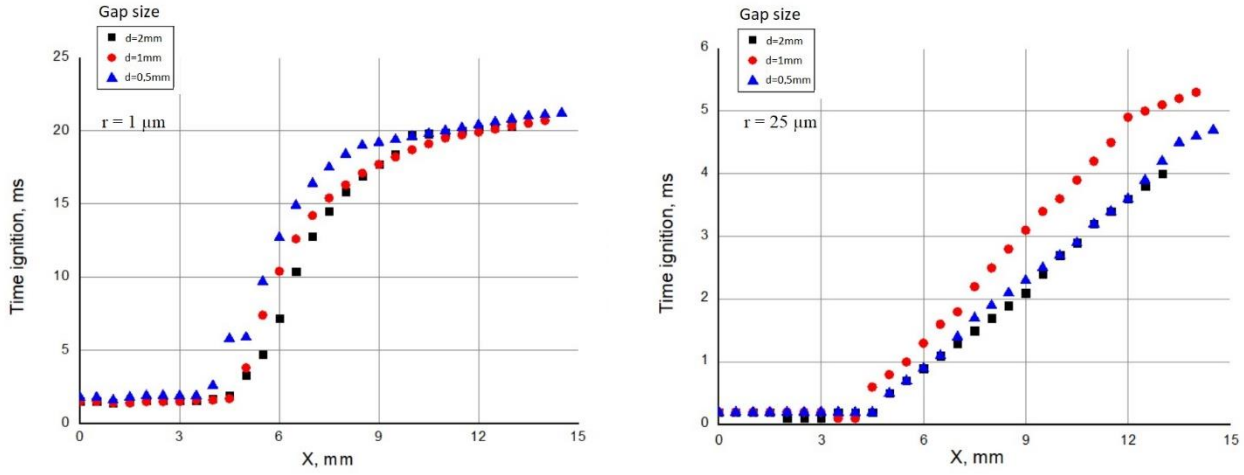

a) b)

Fig.4. Influence of the gap size between the cylindrical surfaces of the cartridge case and the fuel grain on the ignition time of the end part of the fuel grain: ■ – *d*=2mm, ● – *d*=1mm, ▲ –=0.5mm, a) *r* = 1 μm, b) *r* = 25

The speed at which the end surface of the fuel grain is connected to the combustion process, as well as the free volume in the cartridge case, affect the pressure rise rate in the cartridge case. Figure 5 shows the dependence of the average pressure in the cartridge case from time for different values of the cylindrical gap and different particle sizes. After reaching the boosting pressure of the membrane (8 atm), the pressure drops and is set equal to the quasi-static pressure.

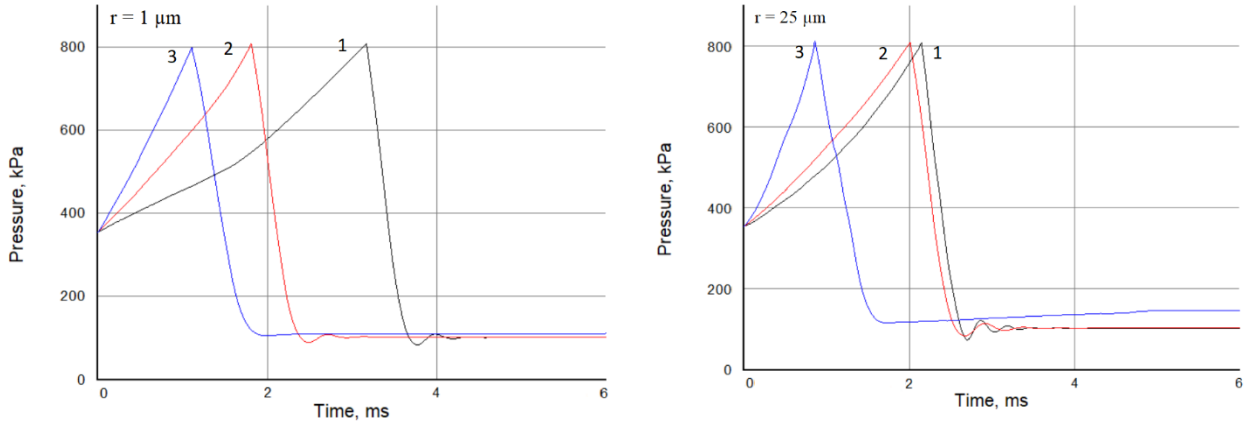

a) b)

Fig.5. Dependence of average volume pressure in the cartridge case on time:
1 - *d*=2mm, 2 - *d*=1mm, 3 - *d*=0.5mm, a) *r* = 1 μm, b) *r* = 25 μm

A reduction of the cylindrical gap and an increasing in particle size leads to fast rising in boosting of pressure and, consequently, to an earlier removal of the membrane. At the same time, a smaller cylindrical gap delays the time of the pressure drop in the cartridge case after the membrane removal, which leads to an increase in the grain launching speed (figure 6).

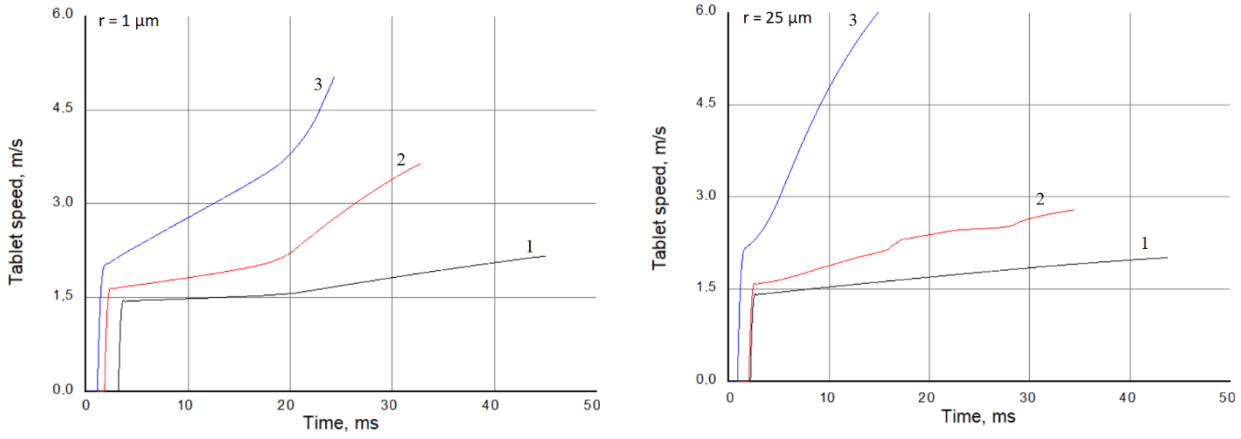

a) b)

Fig.6. Effect of gap size on grain movement speed: 1 - *d*=2mm, 2 - *d*=1mm, *3* - d=0.5mm, a) *r* = 1 μm, b) *r* = 25 μm

An increasing in particle size in the case of a cylindrical gap of 0.5 mm also leads to an increasing in the launching speed of the grain from the cartridge case and does not affect the launching speed for a gap of 2 mm. However, for a 1 mm gap, increasing the particle size reduces the grain ejection rate.

6. Conclusions

Under this study, it was found that the size of the gap between the cylindrical surfaces of the cartridge case and the grain has a significant effect on the ignition process of the end surface of the grain, which is manifested in the fact that increasing the gap size contributes to increasing the temperature grain end surface, and, therefore, leads to decreasing time ignition.

Reducing the particle size leads to increasing ignition time of the grain end part. This dependence is important for designing and creating ignition systems, for example, to achieve certain time characteristics of ignition of different areas of the grain surface.

Reducing the size gap between the cylindrical surfaces of the fuel grain and the cartridge case, and, consequently, the free volume in the cartridge case, leads to increasing in the speed at which the grain leaves the cartridge case.

Obtained results offer the challenge for further research and development in the field of creating more efficient ignition systems. Improved ignition timing and control of the ignition process can lead to increased reliability and efficiency of these systems.

Conflict of interest statement

The authors declare that they have no conflict of interest in relation to this research, whether financial, personal, authorship or otherwise, that could affect the research and its results presented in this paper.

CRediT author statement

Minkov L.L.: Conceptualization, Methodology, Writing - Review & Editing; Gimayeva N.R.: Writing - Original Draft, Visualization, Software. The final manuscript was read and approved by all authors.

Acknowledgments

This work was carried out with financial support from the Ministry of Science and High Education of the Russian Federation (State assignment No. FSMN-2020-0028).

References

1 Vernidub I.I., Puzyrev N.G. *Specialists in explosives, pyrotechnics and ammunition*, 2006. [in Russian]. https://search.rsl.ru/ru/record/01002911196

2 Shidlovskiy A.A., *Fundamentals of Pyrotechnics*, 2021. [in Russian]. https://www.labirint.ru/ books/ 826232/

3 Danilin Yu.G., Nazarov N.A., Novikova N.I. *Explosives, pyrotechnics, means of initiation in the post-war period: People. The science. Production.* 2001. [in Russian]. https://rusneb.ru/catalog/000219_000026_RU_%D0%93%D0%9F%D0%9D%D0%A2%D0%91+%D0%A0%D0%BE%D1%81%D1%81%D0%B8%D0%B8_IBIS_0000277113/

4 Mel'nikov V.E. *Modern pyrotechnics*, 2014. [in Russian]. https://pyrohobby.ru/media/filer/ 86/1a/861aa88a-2ece-4d21-a800-0177eaaacc7e/oglavlenie.pdf

5 Li Q., Liu P., He G. Fluid–solid coupled simulation of the ignition transient of solid rocket motor. *Acta Astronautica*, 2015, Vol. 110, pp.180-190. https://doi.org/10.1016/j.actaastro.2015.01.017

6 Minkov L.L., Shrager E.R., Kiryushkin A.E. Two approaches for simulating the burning surface in gas dynamics. *Key Engineering Materials*, 2016, Vol. 685, pp.114-118. https://doi.org/10.4028, www.scientific.net/ KEM. 685.114

7 Nigmatulin R.I. *Dynamics of Multiphase Media*, 1991, 1, Hemisphere, New York, NY.

8 Li Y., Chen X., Xu J., Zhou Ch., Musa O. Three-dimensional multi-physics coupled simulation of ignition transient in a dual pulse solid rocket motor. *Acta Astronautica*, 2018, Vol. 146, pp.46-65. https://doi.org/10.1016/j.actaastro.2018.01.058

9 Arkhipov V.A., Zolotorev E.A., Orlova M.P., Kozlov N.N., Bondarchuk I.S., Bondarchuk S.S. Mathematical modeling of disposal of the payload fairing of a launch vehicle after completion. *Vestnik Tomskogo gosudarstvennogo universiteta. Matematika i mekhanika*, 2023, Vol.84, pp.52-67. https://doi.org/10.17223/19988621/84/5

10 Goodman T.R. Application of integral methods to transient nonlinear heat transfer. Irvine, T. , Hartnett, J. (Eds), *Advances in Heat Transfer*, Academic Press, New-York, 1964, Vol. 1, pp.51-122. https://doi.org/10.1016/S0065-2717(08)70097-2

11 Menter F.R. Two-Equation Eddy-Viscosity Turbulence Models for Engineering Applications. *AIAA Journal*, 1994, Vol. 32, No. 2, pp.1598-1605. https://doi.org/10.2514/3.12149

12 Sorkin R.Ye., *Theory of intra-chamber processes in solid fuel rocket systems*, 1983, Nauka, Moscow. [in Russian]

13 Wang Y., Zhang X. Numerical investigation on muzzle flow characteristics for small combustion chamber with embedded propelled body. *Structures*, 2023, Vol. 50, pp.1783-1793. https://doi.org/10.1016/j.istruc.2023.03.001

14 Wang Y., Ding Sh., Zhang X. A novel structure to inhibit barrel erosion induced by thermal effects in a propulsion system. *International Communications in Heat and Mass Transfer*, 2023, Vol. 147, No. 106991, pp.1-10. https://doi.org/10.1016/j.icheatmasstransfer.2023.106991

15 Vasquez S.A., Ivanov V.A. A phase coupled method for solving multiphase problems on unstructured meshes, in Proceedings of ASME 2000 Fluids Engineering Division Summer Meeting (ASME FEDSM'00), 2000, paper FEDSM2000 - 11281, pp. 1–6, Boston, MA, USA. https://www.researchgate.net/publication/291857375_A_phase_coupled_method_for_solving_multiphase_problems_on_unstructured_meshes

16 Berezovskaya I.E., Tasmukhanova A.A., Ryspaeva M.Zh., Ospanova Sh.S. Investigation of the influence of liquid fuel injection rate on the combustion process using KIVA–II software. *Eurasian Physical Technical Journal*, 2023, Vol.20, No.3 (45), pp.43-51. https://doi.org/10.31489/2023No3/43-51

17 Komarov I.I., Vegera A.N., Bryzgunov P.A., Makhmutov B.A., Smirnov A.O. Development and research of the topology of cooling baffles for blades of the axial carbon dioxide turbines. *Eurasian Physical Technical Journal*, 2022, Vol.19, No.2(40), pp.48-57. https://doi.org/10.31489/2022No2/48-57

AUTHORS' INFORMATION

Minkov, L.L. - Doctor of Phys. - Math. Sciences, Professor, Mathematical Physics Department, Physics Engineering Faculty, Tomsk State University, Tomsk, Russian Federation; ORCID ID: 0000-0001-6776-6375; lminkov@ftf.tsu.ru

Gimayeva, N.R. - Post graduate student, Physics Engineering Faculty, National Research Tomsk State University, Tomsk, Russian Federation; ORCID ID: 0009-0006-9662-6818; natalia.gimaeva@inbox.ru